AJNR

Age-Related Changes of Cerebral Autoregulation: New Insights with Quantitative T2′-Mapping and Pulsed Arterial Spin-Labeling MR Imaging

M. Wagner, A. Jurcoane, S. Volz, J. Magerkurth, F.E. Zanella, T. Neumann-Haefelin, R. Deichmann, O.C. Singer and E. Hattingen

AJNR Am J Neuroradiol 2012, 33 (11) 2081-2087
doi: https://doi.org/10.3174/ajnr.A3138
http://www.ajnr.org/content/33/11/2081

ORIGINAL RESEARCH

M. Wagner
A. Jurcoane
S. Volz
J. Magerkurth
F.E. Zanella
T. Neumann-Haefelin
R. Deichmann
O.C. Singer
E. Hattingen

Age-Related Changes of Cerebral Autoregulation: New Insights with Quantitative T2′-Mapping and Pulsed Arterial Spin-Labeling MR Imaging

BACKGROUND AND PURPOSE: Cerebral perfusion and O_2 metabolism are affected by physiologic age-related changes. High-resolution motion-corrected quantitative T2′-imaging and PASL were used to evaluate differences in deoxygenated hemoglobin and CBF of the gray matter between young and elderly healthy subjects. Further combined T2′-imaging and PASL were investigated breathing room air and 100% O_2 to evaluate age-related changes in cerebral autoregulation.

MATERIALS AND METHODS: Twenty-two healthy volunteers 60–88 years of age were studied. Two scans of high-resolution motion-corrected T2′-imaging and PASL-MR imaging were obtained while subjects were either breathing room air or breathing 100% O_2. Manual and automated regions of interest were placed in the cerebral GM to extract values from the corresponding maps. Results were compared with those of a group of young healthy subjects previously scanned with the identical protocol as that used in the present study.

RESULTS: There was a significant decrease of cortical CBF ($P < .001$) and cortical T2′ values ($P < .001$) between young and elderly healthy subjects. In both groups, T2′ remained unchanged under hyperoxia compared with normoxia. Only in the younger but not in the elderly group could a significant ($P = .02$) hyperoxic-induced decrease of the CBF be shown.

CONCLUSIONS: T2′-mapping and PASL in the cerebral cortex of healthy subjects revealed a significant decrease of deoxygenated hemoglobin and of CBF with age. The constant deoxyHb level breathing 100% O_2 compared with normoxia in young and elderly GM suggests an age-appropriate cerebral autoregulation. At the younger age, hyperoxic-induced CBF decrease may protect the brain from hyperoxemia.

ABBREVIATIONS: BOLD = blood oxygen level–dependent; deoxyHb = deoxyhemoglobin; GM = gray matter; GM frontoparietal = frontoparietal cortex (automatic ROI); MPRAGE = magnetization-prepared rapid acquisition of gradient echo; OEF = oxygen extraction fraction; PASL = pulsed arterial spin-labeling; rCBF = regional CBF

Brain tissue depends almost exclusively on oxidative phosphorylation; hence, its functional and structural integrity relies on a constant oxygen supply provided by brain perfusion. A close functional coupling between cerebral O_2 metabolism and CBF by cerebral autoregulation satisfies the O_2 demand, even during neuronal activation, and protects the brain from high partial pressures of oxygen.[1] Pathologic change in 1 or both of these parameters or the cerebrovascular autoregulatory mechanism may result in cerebral dysfunction. Chronic arterial hypertension is one of the most important factors affecting cerebrovascular autoregulation.[2] Furthermore, alterations in CBF or in cerebrovascular autoregulation are discussed in neurodegeneration.[3,4] An acute breakthrough of autoregulation may play an important role in acute hypertensive encephalopathy, eclampsia, and in acute brain injury.[5,6]

CBF of the cerebral gray matter decreases with increasing age,[7-15] and the decrease of CBF might be explained by impaired cerebral autoregulation due to changes in endothelial function[16] or, alternatively, by a decrease in cerebral O_2 demand. Degenerative microvascular changes associated with normal aging[17] may also reduce the level of CBF in aging brains.

In the past, O_2 metabolism and CBF were studied with methods having disadvantages such invasiveness (eg, contrast agents, blood samples), radiation exposure, and/or limited spatial resolution (eg, PET).[11,18-20] Noninvasive quantitative MRI can also be used to measure O_2 metabolism and CBF[21-29] and to differentiate physiologic age-related changes from pathologic changes.[28-39]

The BOLD effect[40] describes the dependence of transverse relaxation time of blood water on blood oxygenation. Because the field gradients around erythrocytes increase in the presence of the paramagnetic deoxyHb and result in accelerated spin dephasing, increasing deoxyHb will cause reduced values of the effective transverse relaxation time T2* and thus reduced signal in T2*-weighted images.[37,38] Because T2* is also affected by the transverse relaxation time T2, which is known to increase with age and in almost all cerebral pathologies, the relaxation time T2′ can be calculated from $1 / T2^* - 1 / T2 = 1 / T2'$. T2′ provides mainly information about local concentrations of DeoxyHb.[31,41] In a retrospective study on a 1.5 T scanner, T2, T2′, and T2* values of the white matter, the thal-

Received December 23, 2011; accepted after revision February 29, 2012.

From the Institute of Neuroradiology (M.W., A.J., J.M., F.E.Z., E.H.) and Department of Neurology (T.N.-H., O.C.S.), University Hospital, and Brain Imaging Center (S.V., R.D.), Goethe University Frankfurt am Main, Frankfurt am Main, Germany.

Please address correspondence to Marlies Wagner, MD, Institute of Neuroradiology, Goethe University Hospital, Schleusenweg 2–16, D-60528, Frankfurt am Main, Germany; e-mail: marlies.wagner@kgu.de

http://dx.doi.org/10.3174/ajnr.A3138

ami, and the basal ganglia have already been quantified[31] on the basis of this technique.

Perfusion mapping based on PASL is useful to quantify rCBF.[42]

In this prospective study, we performed high-resolution motion-corrected quantitative T2′-imaging and PASL-MR imaging in elderly healthy volunteers. A preceding study investigating this methodic approach in the gray matter of healthy young subjects suggested that it is accurate to evaluate cerebrovascular autoregulation under hyperoxic conditions (Wagner M, Magerkurth J, Volz S, et al; unpublished data, 2011). The present study investigated the degree to which the CBF of cerebral gray matter decreases with age, whether there is a similar decrease of the oxygen content of the gray matter with age, and whether there are age-related changes of the cerebral autoregulation tested under hyperoxia (inhalation of 100% O_2).

Materials and Methods

Subjects

Twenty-two healthy elderly volunteers (60–88 years of age; median, 66 years) were studied. The protocol was approved by the institutional review board, and informed consent was obtained from each subject. Standardized questionnaires were used to exclude neurologic or psychiatric diseases, diabetes, or untreated hypertension. Following data analysis, 2 subjects had to be excluded due to pronounced motion artifacts.

MR Imaging Examination

Studies were performed on a 3T MR imaging scanner (Magnetom Trio; Siemens, Erlangen, Germany) by using an 8-channel phased-array head coil for signal reception and a body coil for radio-frequency transmission. MR imaging was performed using ear protection; but to avoid artificially low brain metabolism, no further sensory deprivation was used.[11,20] Two scans were obtained, either while subjects were breathing room air or while subjects had been ventilated with 100% O_2 (flow rate 10 l/min) via a close-fitting mask covering the mouth and nose. Because oxygen saturation is known to reach its maximum after approximately 70 seconds,[43] the volunteers were continuously ventilated with 100% oxygen during the entire second series of MR imaging scans, and T2′ and PASL measurements were performed after running an anatomic scan (T1-weighted MPRAGE; duration, 7 minutes, 23 seconds) to ensure an equilibration of the maximum oxygen saturation.

For quantitative T2*-mapping, a multiple gradient-echo sequence with 8 echoes per excitation acquired exclusively under positive readout gradient polarity[44] was used with the following imaging parameters: TE ranging from 10 to 52 ms with a constant increment of 6 ms, TR = 3000 ms, 50 axial sections with 2-mm section thickness, no intersection gap, bandwidth = 300 Hz/pixel, matrix size = 160 × 128 (readout × phase encoding), FOV = 200 × 160 mm^2, isotropic spatial in-plane resolution = 1.25 × 1.25 mm^2, measurement time = 6 minutes 24 seconds. To avoid erroneous T2* values due to distortions of the static magnetic field B0,[45-47] a compensation method was applied[48] on the basis of obtaining B0 distortion maps directly from the complex image data and correcting for TE-dependent image intensity reductions induced by through-plane spin dephasing. The acquisition was repeated with 50% spatial resolution in the phase-encoding direction (duration, 3 minutes 30 seconds), and a special combination of data in *k*-space was used, which was optimized for the suppression of motion-induced artifacts.[41]

Quantitative T2 mapping was based on a series of T2-weighted images with different values of TE (17, 86, 103, 120, 188 ms) by using a TSE sequence. TR had a constant value of 10 seconds, and all geometric parameters (spatial resolution and spatial coverage) were identical to those in the T2*-mapping experiment. Before T2 fitting, the TSE images were coregisterd to the first T2*-weighted image by using the linear registration algorithm implemented in FSL (http://www.fmrib.ox.ac.uk/fsl/fsl/list.html)[49] known as FLIRT.[50]

Data fitting was performed with custom-built programs written in Matlab (MathWorks, Natick, Massachusetts), by using exponential fitting for obtaining maps of T2* and T2. Maps of T2′ were calculated as $1/T2' = 1/T2^* - 1/T2$.

Anatomic imaging was based on a T1-weighted MPRAGE sequence[51] with the following parameters: TR/TE/TI = 2250/2.6/900 ms, whole-brain coverage, isotropic spatial resolution = 1 mm^3, bandwidth = 200 Hz/pixel, duration = 7 minutes, 23 seconds. This dataset was used for segmentation of gray and white matter and automatic definition of ROI. The fitted maps (T2, T2*, and T2′) were linearly coregistered to the T1-weighted anatomical data set using FLIRT.[50]

For quantitative measurement of brain perfusion, 100 pairs of control and tag images were acquired with a PASL technique. The labeling method used was quantitative imaging of perfusion by using a single-subtraction second version with interleaved thin-section TI periodic saturation as described by Luh et al,[52] applying the proximal inversion with a control for an off-resonance-effects labeling scheme, in which arterial spins are labeled by a thick inversion slab proximal to the imaging sections. The scanning parameters were the following: FOV = 22.4 × 22.4 cm, matrix size = 64 × 64, isotropic in-plane resolution = 3.5 × 3.5 mm^2, 5 axial sections of 6 mm each, TR = 2500 ms, TE = 21 ms, TI1/TI1stop/TI2 = 700/13,750/1400 ms. The gap between the tag inversion slab and the first of the imaging sections was 10 mm. The duration was 8 minutes, 20 seconds.

It is known that breathing 100% O_2 reduces the T1 relaxation time in the lung approximately 5%–15% compared with room air inhalation.[53-55] Uematsu et al[56] reported an 11% T1 decrease in the cerebral cortex when subjects were exposed to 100% O_2 in a mouse model studied at a field strength of 9.4T. Considering that hyperoxic-induced T1 relaxation time change in the lung represents an upper limit of T1 change, we used an estimated factor of 10% to correct T1 values before computation of the PASL-based CBF maps under hyperoxic inhalation.

ROIs were manually placed in frontoparietal paramedian cortical structures and in the thalami (Fig 1). GM frontoparietal and whole WM ROIs were also defined following automatic segmentation with SPM8 (http://www.fil.ion.ucl.ac.uk/spm) of the T1-weighted dataset by thresholding the tissue probability maps at 0.95. Due to a low number of sections, only the manually drawn region of interest in the frontoparietal paramedian cortex was defined for the PASL images.

Both manual and automatic ROIs were used as masks to extract T2, T2*, and T2′ values from the corresponding maps. For each region of interest, mean normoxic T2′ and CBF values were extracted by using fslstats, as part of FSL.[49] The results were compared with those of the same parameters assessed under hyperoxic ventilation by using the Wilcoxon signed rank test. Statistical comparison was performed by means of the software R Statistics (http://www.R-project.org).[57] Results were compared with those of the young

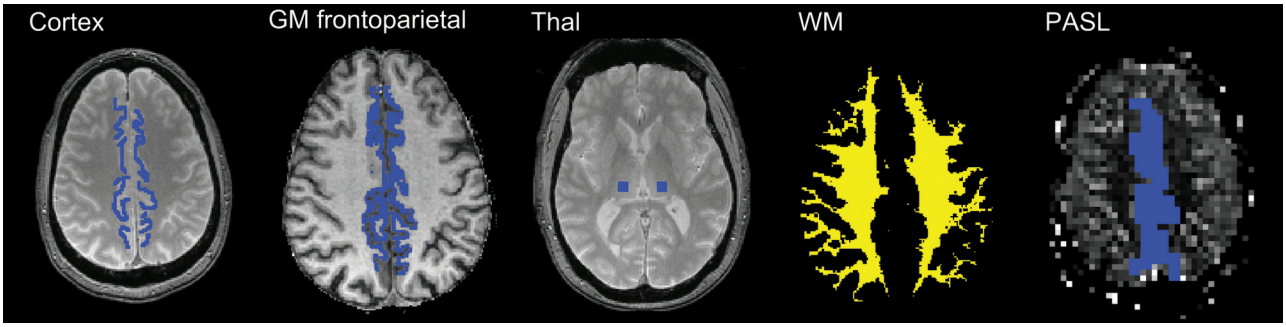

Fig 1. Manually placed ROIs on the first T2*-weighted image (TE = 10 ms) in the frontoparietal paramedian and thalamus. Automatically defined GM frontoparietal and WM ROIs from automatic segmentation. Due to a low number of sections, only the manually drawn region of interest in the frontoparietal paramedian cortex was defined for the PASL images.

Table 1: Parameter values (millisecond, mean ± SD) for room air-breathing (normoxia) and O_2 ventilation (hyperoxia) for both the young and the elderly groups[a]

	Normoxia			Hyperoxia		
Raw Parameter Values	Young	Elderly	*P* Value, Young∼Old	Young	Elderly	*P* Value, Young∼Old
T2′ Cortex	142.5 ± 9.2	124.5 ± 11.6	$P < .001$[b]	138.7 ± 12.2	121.7 ± 9.8	$P < .001$[b]
T2′ GM frontoparietal	126.9 ± 8.4	101 ± 11.3	$P < .001$[b]	124.9 ± 11.4	103.2 ± 8.6	$P < .001$[b]
T2′ Thal	116 ± 13.4	111.6 ± 12.4	$P = .423$	116.5 ± 9.7	111.4 ± 13.1	$P = .477$
T2′ WM	116.3 ± 5.7	103.8 ± 9.4	$P < .001$[b]	117.7 ± 5.8	104.9 ± 5.9	$P < .001$[b]
T2* Cortex	63.2 ± 2.5	60.8 ± 3.7	$P = .074$	62 ± 2.4	60.1 ± 2.8	$P = .07$
T2* GM frontoparietal	59.1 ± 1.7	57.1 ± 2.8	$P = .037$[b]	58.7 ± 2.2	57.4 ± 2.4	$P = .158$
T2* Thal	50.2 ± 2.5	51.4 ± 3.9	$P = .403$	50.3 ± 2.1	51.6 ± 4.6	$P = .255$
T2* WM	51.5 ± 1.2	51.1 ± 2.5	$P = .683$	51.8 ± 0.9	51.2 ± 2.1	$P = .182$
T2 Cortex	121.5 ± 7.8	130.6 ± 13.5	$P = .063$	120.7 ± 6.9	134.7 ± 14.1	$P = .002$[b]
T2 GM frontoparietal	106.6 ± 6.8	113.9 ± 13.4	$P = .063$	105.9 ± 8.4	123.5 ± 15.5	$P = .001$[b]
T2 Thal	91.8 ± 2.3	100.3 ± 9.5	$P < .001$[b]	92 ± 2.5	98.4 ± 7.2	$P = .005$[b]
T2 WM	93.4 ± 1.7	101 ± 5.1	$P < .001$[b]	93.7 ± 2	102.6 ± 4.9	$P < .001$[b]
PASL	61.5 ± 9.9	43.4 ± 12.1	$P < .001$[b]	56.2 ± 8.5	41.9 ± 12.6	$P = .001$[b]

Note:—Thal indicates thalamus; Cortex, frontoparietal paramedian.
[a] "Cortex" is defined as the manual ROI, "GM frontoparietal" as the automated ROI, "WM" as the automated whole supratentorial white matter, and "Thal" as the manual thalamic ROI (Fig 1).
[b] Significant.

healthy volunteers previously described, a study also approved by the local ethics committee.

Results

Significant differences between elderly and younger (Table 1) healthy volunteers were found in both cortical CBF ($P < .001$) and T2′ values of cortical GM (manual and automatic region-of-interest modalities, both $P < .001$) and WM ($P < .001$) under normoxic conditions. We found a significant CBF decrease ($P < .001$) of 30% from younger to elderly volunteers (Fig 2). While cortical T2* values changed as a trend (manual region of interest, $P = .074$) or significantly (automated region of interest, $P = .037$) and T2* values of the white matter remained unchanged, T2′ of both the cortex and white matter decreased highly significantly ($P < .001$ each) due to the increase of cortical (as a trend, $P = .063$) and white matter (highly significantly, $P < .001$) T2 values with age ($1 / T2' = 1 / T2^* - 1 / T2$), though this effect was less pronounced than the CBF reduction.

In the thalami, only T2 increased significantly ($P = .001$) with age, while T2* and T2′ remained unchanged.

In both the younger and older subjects, T2′ (Fig 3) and T2* remained unchanged under hyperoxia compared with room-air breathing, while only in the older group did T2 increase significantly in the cortex ($P = .033$ and $P = .005$) and white matter ($P = .04$) under hyperoxia (Tables 1 and 2). While in the younger group the CBF had decreased significantly ($P = .02$) under hyperoxia, in the older group, the CBF showed only a nonsignificant decrease compared with room-air breathing (Fig 4).

Discussion

We have used PASL for measuring CBF and T2′ imaging for determining the deoxyHb content of the cerebral cortex in 2 groups of healthy subjects with different ages. Compared with the mean cortical CBF values of young healthy (20–34 years) individuals, we found a CBF decrease of approximately 30% (from 61 to 43 mL/100 g/min) in the elderly (61–89 years). The CBF decrease in the elderly is most likely the result of physiologic age-related changes leading to neuronal shrinkage and/or degenerative change of the microvasculature.[7-9,11-15] The CBI decrease is accompanied by a significant decrease of the cortical T2′ values (124.5 versus 142.5 ms for the younger group), which indicates increasing cortical deoxyHb content with age. The deoxyHb content depends on the CBV and the deoxyHb fraction in the blood. Increase in deoxyHb content can be attributed to reduced flow at constant oxygen consumption, leading to an increased oxygen extraction fraction. While Pantano et al[14] found an increasing trend of the OEF of 7% in elderly healthy men compared with

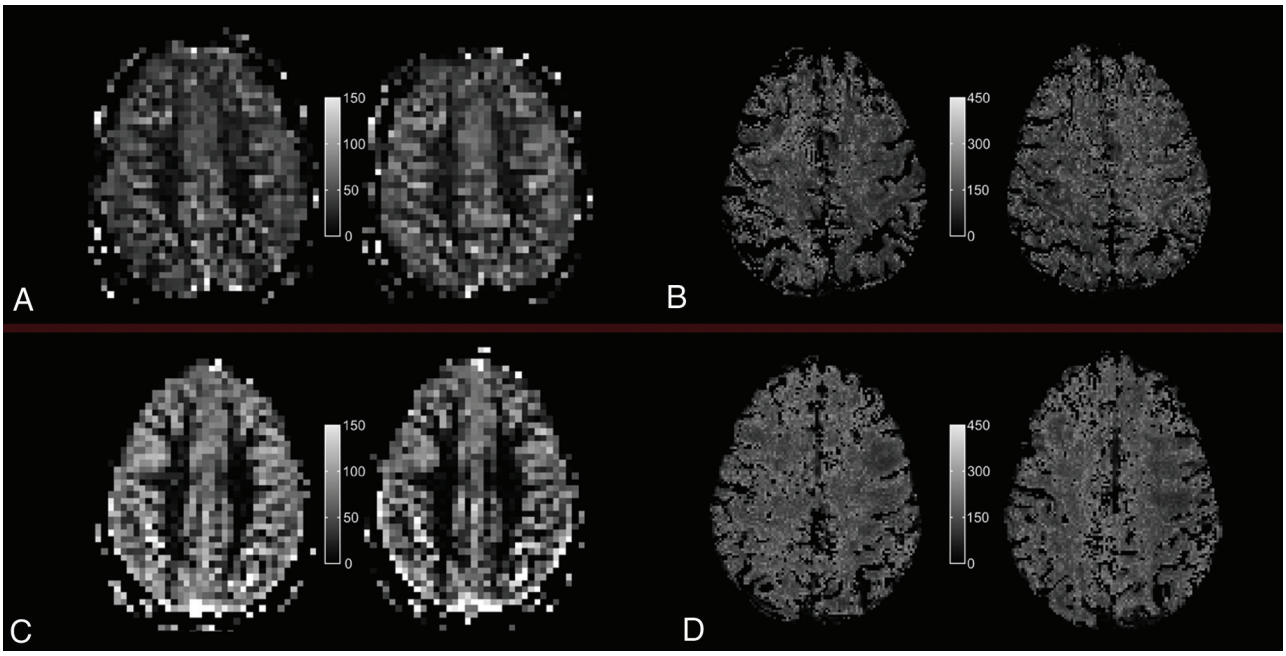

Fig 2. Quantitative PASL-based CBF map (*A* and *C*) and T2′ map (*B* and *D*) under room-air breathing (left) and under hyperoxic ventilation (right) for a single section and 1 representative elderly subject (top, *A* and *B*) and a representative young subject (bottom, *C* and *D*), respectively.

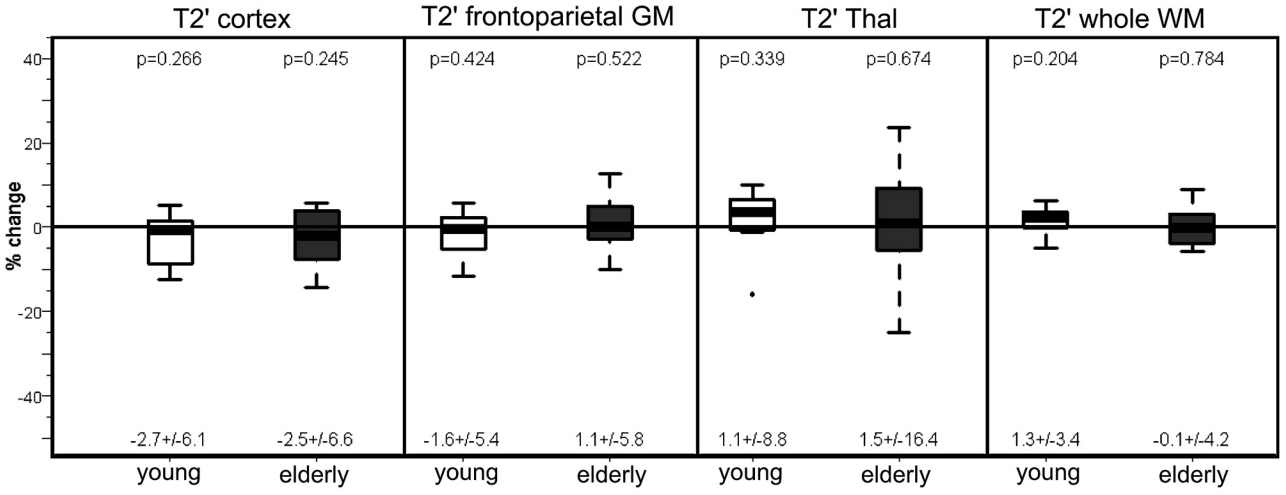

Fig 3. Percentage change of T2′ relaxation times on O_2 administration in the 2 subject groups (young and elderly) in all the investigated regions. For each group, mean ± SD are given under each boxplot, and *P* values of the difference from zero are provided above the boxplot.

younger subjects, Leenders et al[11] did not find any changes of the OEF with age by using PET. The difference in our results might be due to reduced partial volume effects of white matter and CSF for the quantitative MRI method.

Under hyperoxia, the CBF in young subjects decreased significantly ($P = .02$). In contrast to the young adults, the elderly group revealed only a trend toward decreased CBF on hyperoxia. However, cerebral autoregulation was still sufficient because the deoxyHb content remained constant. The relationship between a decreased CBF and an increased OEF of the aging brain[11,12,14,18,58] might hint at a latent CBF/O_2 undersupply. In this case, the oxygen surplus after inhalation of 100% O_2 can be compensated by increased oxygen consumption. The rather luxurious perfusion of younger brains might explain the significant cortical CBF decrease under hyperoxia. Additional O_2 supply, which cannot be compensated by increased consumption, leads to reactive vasoconstriction to prevent pathologic O_2 concentrations in the brain.

A recent review[16] showed a significant decrease of the vasoreactivity in healthy elderly volunteers. It can be speculated that the age-dependent decrease in CBF shifts the autoregulation under hyperoxia from vasoconstriction to increasing oxygen consumption.

The mean rCBF values of 43 ± 12 mL/100 g/min measured by PASL in the paramedian frontoparietal cortex of elderly healthy subjects are in line with the results of previous studies by using the same method.[59] Our results are also consistent with those of several other previous studies showing an age-dependent CBF decrease between 0.5% and 0.7% per year,[7-15] with a high range of interindividual variation.[11,12,14,58,59] Due to cortical atrophy in the elderly, the limited spatial resolution of PASL ($3.5 \times 3.5 \times 6$ mm^3) might lead to increased partial

Table 2: Percentage parameter change (mean ± SD) on administration of O_2 for the young and elderly groups

$\Delta = (O_2/\text{no } O_2 - 1) \times 100$	Young	*P* Value, Δ Young = 0	Elderly	*P* Value, Δ Elderly = 0
T2′ Cortex O_2	1.1 ± 8.8	*P* = .34	−2.5 ± 6.6	*P* = .245
T2′ GM frontoparietal O_2	0.0 ± 4.4	*P* = .73	1.1 ± 5.8	*P* = .522
T2′ Thal O_2	−1.8 ± 4.0	*P* = .52	1.5 ± 16.4	*P* = .674
T2′ WM O_2	0.3 ± 3.5	*P* = .68	−0.1 ± 4.2	*P* = .784
T2* Cortex O_2	0.4 ± 2.4	*P* = .3	−0.8 ± 4.1	*P* = .498
T2* GM frontoparietal O_2	0.7 ± 1.4	*P* = .09	0.3 ± 3.6	*P* = .452
T2* Thal O_2	0.3 ± 3.3	*P* = .91	1.4 ± 9.6	*P* = .756
T2* WM O_2	−0.7 ± 4.3	*P* = .68	−0.2 ± 2.5	*P* = .596
T2 Cortex O_2	0.4 ± 1.5	*P* = .38	4.1 ± 7.6	*P* = .033[a]
T2 GM frontoparietal O_2	−8.1 ± 8.2	*P* = .01[a]	8.9 ± 13.8	*P* = .005[a]
T2 Thal O_2	0.3 ± 10.4	*P* = .57	−0.8 ± 6.4	*P* = .812
T2 WM O_2	−1.9 ± 3.4	*P* = .11	1.8 ± 3.3	*P* = .04[a]
PASL_O_2	−2.4 ± 3.0	*P* = .02[a]	−2.5 ± 16.5	*P* = .539

Note:—Thal indicates thalamus; Cortex, frontoparietal paramedian.
[a] Significant.

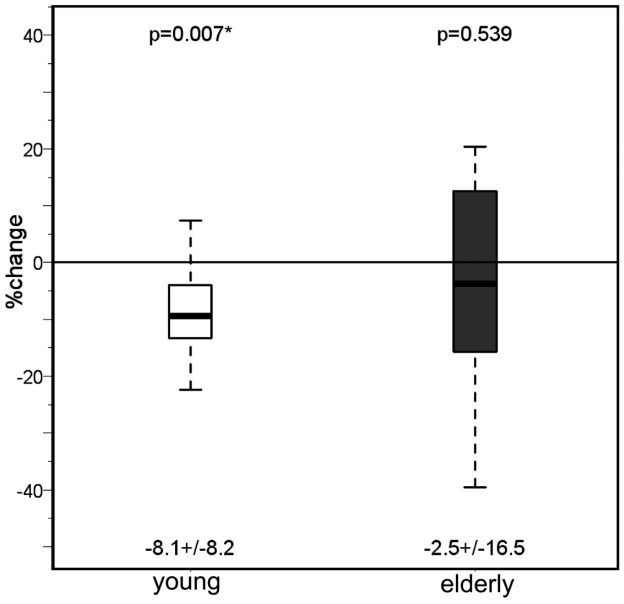

Fig 4. Values of the cerebral blood flow measured with PASL under normoxia and hyperoxia in both the young and the elderly groups. Mean ± SD are given under each boxplot, and *P* values of the difference between the groups are provided above the boxplots.

volume effects regarding white matter and CSF and cause a higher SD of CBF values compared with those in the younger group (Fig 2).[11,12,28,34,58-62] Furthermore, spin-labeling methods presume an orthogonal caudocranial blood flow. In older patients, however, the increasing transit time of the perforating and end arterioles may occur on the basis of arteriosclerotic changes resulting in an overestimation of hypoperfusion.[12,59] Furthermore, cerebrovascular sequelae of age-related increase in blood pressure or of asymptomatic ICA stenoses may decrease CBF in elderly subjects, but patients with known and symptomatic neurologic and cardiovascular diseases were excluded from the study. A potential influence of unknown vascular changes on age-related CBF decrease should not be overestimated because asymptomatic severe ICA stenosis is very rare in the healthy population[63] and elderly individuals frequently undergo checkups of blood pressure.

T2′ values are influenced not only by the deoxyHb content but also by paramagnetic iron deposits in the tissue. The iron content of the cortex and of the thalamus is continuously increasing in young adolescents. Beyond the age of approximately 35 years, there is no more increase of cortical and thalamic iron deposits, but in contrast, they may even decrease. Consequently, the differences of the age-dependent T2′ values are not attributed to a difference of iron content but to the higher deoxyHb content in elderly subjects.[21,29,62,64]

This study stresses the requirement to calculate T2-corrected T2* values (T2′). We found an age-dependent increase of the T2 relaxation times in both gray and white matter structures, with a significant increase in the thalami and white matter. The age-dependent changes of the T2 time of the cerebral white matter are widely investigated.[9,15,17,26,32,34,61,64,65-70] Beyond adolescence, there is a re-increase of the T2 time in the cerebral white matter with age due to white matter degeneration and an increased water content.[9,15,17,26,34,61,66-70] However, there are only a few data concerning age-dependent T2 changes of the gray matter. Similar to our results, Siemonsen et al[31] could also quantify an age-dependent increase of T2 in the thalamus, and Autti et al[71,72] qualitatively revealed at least a plateau of the T2 signal in the thalamus visually after a continuous signal decrease until middle adolescence.

The T2 increase of the paramedian frontoparietal cortex may also result from the age-dependent increase of the cortical water content as a consequence of the neuronal shrinkage.[25] An increase of the water content and a decreasing attenuation of macromolecules with age were also determined from diffusion-weighted techniques and magnetization-transfer contrast imaging.[28,34,73] While we could reveal a T2 effect of oxygen in the cerebral cortex and white matter of elderly subjects, this could not be shown in young subjects.

Conclusions

Quantitative MR imaging with high-resolution T2′ mapping and PASL-based CBF mapping demonstrated an age-dependent increase of deoxyHb in the cerebral cortex, while the cortical CBF decreased with age. In both young and elderly healthy subjects, the content of deoxyHb remained constant under hyperoxic inhalation compared with normoxia, but only the younger group showed a significant CBF decrease under hyperoxia. These results suggest an age-appropriate ce-

rebral autoregulation in young and elderly brains, whereas at a younger age, hyperoxic-induced vasoconstriction protects the brain against hyperoxemia.

Acknowledgments

We thank Dr Ulrich Pilatus for editing the manuscript.

Disclosures: Steffen Volz—*RELATED*: *Grant*: support to Brain Imaging Center, Frankfurt: Bundesministerium für Bildung und Forschung (Germany): DLR 01GO0203; Deutsche Forschungsgemeinschaft (Germany): ZA 233/1–1;* *UNRELATED*: *Grants/Grants Pending*: public funding: Land of Hesse, Germany: LOEWE Research grant "Neuronale Koordination Forschungsschwerpunkt Frankfurt," since 2011.* Ralf Deichmann—*RELATED*: *Grant*: support to Brain Imaging Center, Frankfurt: Bundesministerium für Bildung und Forschung (Germany): DLR 01GO0203; Deutsche Forschungsgemeinschaft (Germany): ZA 233/1–1,* *UNRELATED*: *Grants/Grants Pending*: public funding: Land of Hesse, Germany: LOEWE Research grant "Neuronale Koordination Forschungsschwerpunkt Frankfurt," since 2011;* *Royalties*: published book chapters: 1) Deichmann R: "Principles of MRI and Functional MRI. " In: Filippi M, ed. *fMRI Techniques and Protocols*. Heidelberg: Humana Press, Springer, 2009; 2) Deichmann R, Noeth U, Weiskopf N. "The Basics of Functional Magnetic Resonance Imaging." In: Mulert C, Lemieux L, eds. *EEG-fMRI*. Heidelberg: Springer, 2010; (so far no royalties paid); *Travel/Accommodations/Meeting Expenses Unrelated to Activities Listed:* travel expenses for invited lectures given at the following nonprofit organizations: 2010: Max-Delbrück-Center, Berlin/Buch, Germany; 2010: Wellcome Trust Centre for Neuroimaging, Institute of Neurology, UCL, London, UK; 2010: University of Tübingen, Germany; 2011: Research Center Jülich, Germany; 2011: University of Liege, Belgium. *Money paid to the institution.

References

1. Johnston AJ, Steiner LA, Gupta AK, et al. **Cerebral oxygen vasoreactivity and cerebral tissue oxygen reactivity.** *Br J Anaesth* 2003;90:774–86
2. Immink RV, van den Born BJ, van Montfrans GA, et al. **Impaired cerebral autoregulation in patients with malignant hypertension.** *Circulation* 2004;110:2241–45
3. Bateman GA, Levi CR, Schofield P, et al. **Quantitative measurement of cerebral haemodynamics in early vascular dementia and Alzheimer's disease.** *J Clin Neurosci* 2006;13:563–68
4. Cantin S, Villien M, Moreaud O, et al. **Impaired cerebral vasoreactivity to CO2 in Alzheimer's disease using BOLD fMRI.** *Neuroimage* 2011;58:579–87
5. Lee SY, Dinesh SK, Thomas J. **Hypertension-induced reversible posterior leukoencephalopathy syndrome causing obstructive hydrocephalus.** *J Clin Neurosci* 2008;15:457–59
6. Armstead WM, Kiessling JW, Kofke WA, et al. **Impaired cerebral blood flow autoregulation during posttraumatic arterial hypotension after fluid percussion brain injury is prevented by phenylephrine in female but exacerbated in male piglets by extracellular signal-related kinase mitogen-activated protein kinase upregulation.** *Crit Care Med* 2010;38:1868–74
7. Meguro K, Hatazawa J, Yamaguchi T, et al. **Cerebral circulation and oxygen metabolism associated with subclinical periventricular hyperintensity as shown by magnetic resonance imaging.** *Ann Neurol* 1990;28:378–83
8. Yamauchi H, Fukuyama H, Yamaguchi S, et al. **High-intensity area in the deep white matter indicating hemodynamic compromise in internal carotid artery occlusive disorders.** *Arch Neurol* 1991;48:1067–71
9. Fazekas F, Niederkorn K, Schmidt R, et al. **White matter signal abnormalities in normal individuals: correlation with carotid ultrasonography, cerebral blood flow measurements, and cerebrovascular risk factors.** *Stroke* 1988;19:1285–88
10. Kety SS. **Human cerebral blood flow and oxygen consumption as related to aging.** *J Chronic Dis* 1956;3:478–86
11. Leenders KL, Perani D, Lammertsma AA, et al. **Cerebral blood flow, blood volume and oxygen utilization: normal values and effect of age.** *Brain* 1990;113:27–47
12. Parkes LM, Rashid W, Chard DT, et al. **Normal cerebral perfusion measurements using arterial spin labeling: reproducibility, stability, and age and gender effects.** *Magn Reson Med* 2004;51:736–43
13. Martin AJ, Friston KJ, Colebatch JG, et al. **Decreases in regional cerebral blood flow with normal aging.** *J Cereb Blood Flow Metab* 1991;11:684–89
14. Pantano P, Baron JC, Lebrun-Grandié P, et al. **Regional cerebral blood flow and oxygen consumption in human aging.** *Stroke* 1984;15:635–41
15. Iseki K, Hanakawa T, Hashikawa K, et al. **Gait disturbance associated with white matter changes: a gait analysis and blood flow study.** *Neuroimage* 2010;49:1659–66
16. Seals DR, Jablonski KL, Donato AJ. **Aging and vascular endothelial function in humans.** *Clin Sci (Lond)* 2011;120:357–75
17. Moody DM, Brown WR, Challa VR, et al. **Cerebral microvascular alterations in aging, leukoaraiosis, and Alzheimer's disease.** *Ann N Y Acad Sci* 1997;826:103–16
18. Kety SS, Schmidt CF. **The nitrous oxygen method for quantitative determination of cerebral blood flow in man: theory, procedure and normal values.** *J Clin Invest* 1948;27:476–83
19. Amano T, Meyer JS, Okabe T, et al. **Cerebral vasomotor responses during oxygen inhalation: results in normal aging and dementia.** *Arch Neurol* 1983;40:277–82
20. Duara R, Margolin RA, Robertson-Tchabo EA, et al. **Cerebral glucose utilization, as measured with positron emission tomography in 21 resting healthy men between the ages of 21 and 83 years.** *Brain* 1983;106:761–75
21. Aquino D, Bizzi A, Grisoli M, et al. **Age-related iron deposition in the basal ganglia: quantitative analysis in healthy subjects.** *Radiology* 2009;252:165–72
22. Drayer BP. **Imaging of the aging brain. Part I. Normal findings.** *Radiology* 1988;166:785–96
23. Drayer BP. **Basal ganglia: significance of signal hypointensity on T2-weighted MR images.** *Radiology* 1989;173:311–12
24. Pujol J, Junqué C, Vendrell P, et al. **Biological significance of iron-related magnetic resonance imaging changes in the brain.** *Arch Neurol* 1992;49:711–17
25. Langkammer C, Krebs N, Goessler W, et al. **Quantitative MR imaging of brain iron: a postmortem validation study.** *Radiology* 2010;257:455–62
26. Fazekas F, Chawluk JB, Alavi A, et al. **MR signal abnormalities at 1.5 T in Alzheimer's dementia and normal aging.** *AJR Am J Roentgenol* 1987;149:351–56
27. Fazekas F, Alavi A, Chawluk JB, et al. **Comparison of CT, MR, and PET in Alzheimer's dementia and normal aging.** *J Nucl Med* 1989;30:1607–15
28. Inglese M, Ge Y. **Quantitative MRI: hidden age-related changes in brain tissue.** *Top Magn Reson Imaging* 2004;15:355–63
29. Bartzokis G, Tishler TA, Shin IS, et al. **Brain ferritin iron as a risk factor for age at onset in neurodegenerative diseases.** *Ann N Y Acad Sci* 2004;1012:224–36
30. Rivkin MJ, Wolraich D, Als H, et al. **Prolonged T*2 values in newborn versus adult brain: Implications for fMRI studies of newborns.** *Magn Reson Med* 2004;51:1287–91
31. Siemonsen S, Finsterbusch J, Matschke J, et al. **Age-dependent normal values of T2* and T2′ in brain parenchyma.** *AJNR Am J Neuroradiol* 2008;29:950–55
32. Speck O, Ernst T, Chang L. **Biexponential modeling of multigradient-echo MRI data of the brain.** *Magn Reson Med* 2001;45:1116–21
33. Donahue MJ, Blicher JU, Østergaard L, et al. **Cerebral blood flow, blood volume, and oxygen metabolism dynamics in human visual and motor cortex as measured by whole-brain multi-modal magnetic resonance imaging.** *J Cereb Blood Flow Metab* 2009;29:1856–66
34. Benedetti B, Charil A, Rovaris M, et al. **Influence of aging on brain gray and white matter changes assessed by conventional, MT, and DT MRI.** *Neurology* 2006;66:535–39
35. Brooks DJ, Luthert P, Gadian D, et al. **Does signal-attenuation on high-field T2-weighted MRI of the brain reflect regional cerebral iron deposition? Observations on the relationship between regional cerebral water proton T2 values and iron levels.** *J Neurol Neurosurg Psychiatry* 1989;52:108–11
36. Falangola MF, Dyakin VV, Lee SP, et al. **Quantitative MRI reveals aging-associated T2 changes in mouse models of Alzheimer's disease.** *NMR Biomed* 2007;20:343–51
37. Thulborn KR, Waterton JC, Matthews PM, et al. **Oxygenation dependence of the transverse relaxation time of water protons in whole blood at high field.** *Biochim Biophys Acta* 1982;714:265–70
38. Thulborn KR. **My starting point: the discovery of an NMR method for measuring blood oxygenation using the transverse relaxation time of blood water.** *Neuroimage* 2012;62:589–93
39. Evans AC. **Brain Development Cooperative Group: the NIH MRI study of normal brain development.** *Neuroimage* 2006:30:184–202
40. Ogawa S, Lee TM, Kay AR, et al. **Brain magnetic resonance imaging with contrast dependent on blood oxygenation.** *Proc Natl Acad Sci U S A* 1990;87:9868–72
41. Magerkurth J, Volz S, Wagner M, et al. **Quantitative T*(2)-mapping based on multi-slice multiple gradient echo FLASH imaging: retrospective correction for subject motion effects.** *Magn Reson Med* 2011;66:989–97
42. Williams DS, Detre JA, Leigh JS, et al. **Magnetic resonance imaging of perfusion using spin inversion of arterial water.** *Proc Natl Acad Sci U S A* 1992;89:212–16
43. Losert C, Peller M, Schneider P, et al. **Oxygen-enhanced MRI of the brain.** *Magn Res Med* 2002;48:271–77
44. Ericsson A, Weis J, Hemmingsson A, et al. **Measurements of magnetic field variations in the human brain using a 3D-FT multiple gradient echo technique.** *Magn Reson Med* 1995;33:171–77
45. Ordidge RJ, Gorell JM, Deniau JC, et al. **Assessment of relative brain iron concentrations using T2-weighted and T2*-weighted MRI at 3 Tesla.** *Magn Reson Med* 1994;32:335–41
46. Fernandez-Seara MA, Wehrli FW. **Postprocessing technique to correct for background gradients in image-based R*(2) measurements.** *Magn Reson Med* 2000;44:358–66
47. Yang QX, Williams GD, Demeure RJ, et al. **Removal of local field gradient artifacts in T2*-weighted images at high fields by gradient-echo slice excitation profile imaging.** *Magn Reson Med* 1998;39:402–09

48. Baudrexel S, Volz S, Preibisch C, et al. **Rapid single-scan T2*-mapping using exponential excitation pulses and image-based correction for linear background gradients.** *Magn Reson Med* 2009;62:263–68
49. Smith SM, Jenkinson M, Woolrich MW, et al. **Advances in functional and structural MR image analysis and implementation as FSL.** *Neuroimage* 2004;23:S208–19
50. Jenkinson M, Bannister P, Brady M, et al. **Improved optimization for the robust and accurate linear registration and motion correction of brain images.** *Neuroimage* 2002;17:825–41
51. Mugler JP 3rd, Brookeman JR. **Three-dimensional magnetization-prepared rapid gradient-echo imaging (3D MP RAGE).** *Magn Reson Med* 1990;15:152–57
52. Luh WM, Wong EC, Bandettini PA, et al. **QUIPSS II with thin-slice TI1 periodic saturation: a method for improving accuracy of quantitative perfusion imaging using pulsed arterial spin labeling.** *Magn Reson Med* 1999;41:1246–54
53. Jakob PM, Hillenbrand CM, Wang T, et al. **Rapid quantitative lung 1H T1 mapping.** *J Magn Reson Imaging* 2001;14:795–99
54. Edelman RR, Hatabu H, Tadamura E, et al. **Noninvasive assessment of regional ventilation in the human lung using oxygen-enhanced magnetic resonance imaging.** *Nat Med* 1996;2:1236–39
55. Beer M, Stäb D, Oechsner M, et al. **Oxygen-enhanced functional MR lung imaging.** *Radiologe* 2009;49:732–38
56. Uematsu H, Takahashi M, Hatabu H, et al. **Changes in T1 and T2 observed in brain magnetic resonance imaging with delivery of high concentrations of oxygen.** *J Comput Assist Tomogr* 2007;31:662–65
57. R Foundation For Statistical Computing R Development Core Team. *R: A Language and Environment for Statistical Computing*. Vienna, Austria: R Foundation for Statistical Computing; 2008
58. Akiyama H, Meyer JS, Mortel KF, et al. **Normal human aging: factors contributing to cerebral atrophy.** *J Neurol Sci* 1997;152:39–49
59. Lee C, Lopez OL, Becker JT, et al. **Imaging cerebral blood flow in the cognitively normal aging brain with arterial spin labeling: implications for imaging of neurodegenerative disease.** *J Neuroimaging* 2009;19:344–52
60. Terry RD, DeTeresa R, Hansen LA. **Neocortical cell counts in normal human adult aging.** *Ann Neurol* 1987;21:530–39
61. Rosano C, Sigurdsson S, Siggeirsdottir K, et al. **Magnetization transfer imaging, white matter hyperintensities, brain atrophy and slower gait in older men and women.** *Neurobiol Aging* 2010;31:1197–204
62. Rodrigue KM, Haacke EM, Raz N. **Differential effects of age and history of hypertension on regional brain volumes and iron.** *Neuroimage* 2011;54:750–59
63. de Weerd M, Greving JP, Hedblad B, et al. **Prevalence of asymptomatic carotid artery stenosis in the general population: an individual participant data meta-analysis.** *Stroke* 2010;41:1294–97
64. Hallgren B, Sourander P. **The effect of age on the non-haemin iron in the human brain.** *J Neurochem* 1958;3:41–51
65. Ding XQ, Kucinski T, Wittkugel O, et al. **Normal brain maturation characterized with age-related T2 relaxation times: an attempt to develop a quantitative imaging measure for clinical use.** *Invest Radiol* 2004;39:740–46
66. Marshall VG, Bradley WG Jr, Marshall CE, et al. **Deep white matter infarction: correlation of MR imaging and histopathologic findings.** *Radiology* 1988;167:517–22
67. Awad IA, Spetzler RF, Hodak JA, et al. **Incidental subcortical lesions identified on magnetic resonance imaging in the elderly. I. Correlation with age and cerebrovascular risk factors.** *Stroke* 1986;17:1084–89
68. Braffman BH, Zimmerman RA, Trojanowski JQ, et al. **Brain MR: pathologic correlation with gross and histopathology. 2. Hyperintense white-matter foci in the elderly.** *AJR Am J Roentgenol* 1988;151:559–66
69. Braffman BH, Zimmerman RA, Trojanowski JQ, et al. **Brain MR: pathologic correlation with gross and histopathology. 1. Lacunar infarction and Virchow-Robin spaces.** *AJR Am J Roentgenol* 1988;151:551–58
70. Breger RK, Yetkin FZ, Fischer ME, et al. **T1 and T2 in the cerebrum: correlation with age, gender, and demographic factors.** *Radiology* 1991;181:545–47
71. Autti T, Raininko R, Vanhanen SL, et al. **MRI of the normal brain from early childhood to middle age. I. Appearances on T2- and proton density-weighted images and occurrence of incidental high-signal foci.** *Neuroradiology* 1994;36:644–48
72. Autti T, Raininko R, Vanhanen SL, et al. **MRI of the normal brain from early childhood to middle age. II. Age dependence of signal intensity changes on T2-weighted images.** *Neuroradiology* 1994;36:649–51
73. Nusbaum AO, Tang CY, Buchsbaum MS, et al. **Regional and global changes in cerebral diffusion with normal aging.** *AJNR Am J Neuroradiol* 2001;22:136–42